RECENT CHARM PRODUCTION RESULTS FROM THE FERMILAB FIXED-TARGET EXPERIMENTS E791, SELEX, AND FOCUS

KEVIN STENSON
Department of Physics & Astronomy,
Vanderbilt University, Nashville, TN, USA

Production results are presented from three Fermilab fixed-target charm production experiments, E791, SELEX, and FOCUS which took data with π^-, $p/\Sigma^-/\pi^-$, and γ beams, respectively. The results include measurements of production asymmetries, singly and doubly differential cross sections, and total forward cross sections. Some comparisons to Pythia and next-to-leading order predictions are also made.

1 Introduction

Charm production can be factorized into three parts. The first part is composed of the parton distribution functions (PDF's) which provide information about the flavor and momentum content of the incoming partons. These PDF's are generally derived from deep inelastic scattering data and prompt photon or lepton data. The parton interaction which produces a $c\bar{c}$ pair is governed by the short distance (high Q^2) QCD interaction. Since this interaction takes place at a scale on the order of the charm quark mass ($\sim$1.5 GeV) which is above the QCD scale $\Lambda_{QCD} \sim 0.3$ GeV, this process should be calculable by perturbative QCD but perhaps not too reliably since 1.5 GeV $\not\gg$ 0.3 GeV. The third and final part of the production involves the fragmentation of the charm quarks into charm hadrons. This occurs at the QCD scale and is therefore incalculable by perturbative QCD. In addition, since the charm quarks are tied by color strings to the remnants of the beam and/or target hadrons, the simple Peterson fragmentation prescription is not expected to work well. A more involved fragmentation scheme such as the Lund string fragmentation model may be able to model these effects. By accumulating experimental measurements of various production asymmetries, differential cross sections, and total cross sections using a variety of beams and beam energies, it should be possible to pin down some of the parameters in the theories and eventually test QCD. Presented here are some results which might help us in this quest.

2 Experiments

By measuring various charm production properties we hope to arrive at a coherent picture of charm production and perhaps test QCD. The goals of the three experiments discussed here, E791, SELEX, and FOCUS, are very similar; high-statistics measurements of production and decay properties of charm particles. For SELEX, the emphasis is on forward production and charm baryons while E791 and FOCUS are more general purpose experiments working in the low x_F region. E791 utilized a 500 GeV π^- beam impinging on one platinum and four diamond targets. SELEX used 600 GeV Σ^-/π^- and 540 GeV p beams on two copper and three carbon targets. FOCUS used a photon beam with an average energy of 180 GeV and four BeO targets. Downstream of the targets, E791, SELEX, and FOCUS performed precision tracking and vertexing with 17, 38, and 16 silicon strip planes, respectively. The experiments also used wire chambers and 2-3 magnets for tracking and momentum measurements. While E791 (FOCUS) used 2 (3) threshold Čerenkov counters, SELEX employed a ring imaging Čerenkov counter. E791 and FOCUS used calorimeter information to trigger on hadronic events slightly enriched in charm. SELEX used a more aggressive online vertex trigger based on miss distance. E791 took data in 1991 while SELEX and FOCUS ran in 1996/7.

3 Asymmetries

The asymmetries described here are the production asymmetries of a particle versus its antiparticle either integrated or as a function of kinematic variables such as p_T^2 or $x_F \equiv p_L^*/p_{L_{max}}^*$. These asymmetries are quite interesting because they are expected to be nearly zero for charm quark production. Therefore, the very existence of an asymmetry gives information about the hadronization process, which is further elucidated by measuring the magnitude and kinematic dependence of the effect.

Table 1: "Leadingness" (quarks in common between the beam/target and charm hadron) for various beams/targets and charm hadrons.

Beam	$\mathbf{\Lambda_c^+(cud)}$	$\mathbf{\Lambda_c^-(\bar{c}\bar{u}\bar{d})}$	$\mathbf{D^+(c\bar{d})}$	$\mathbf{D^-(\bar{c}d)}$
$\pi^-(\bar{u}d)$	d	$\bar{u}$	nonleading	d
$\Sigma^-(dds)$	d	nonleading	nonleading	d
$p(uud)$	ud	nonleading	nonleading	d
$n(udd)$	ud	nonleading	nonleading	d

One source of asymmetries may be the fragmentation of the color string between the charm quark and the beam/target fragments. As shown in Table 1, a $D^-(\bar{c}d)$ meson with a d quark in common with the $\pi^-(\bar{u}d)$ beam can come from a coalescence of a π^- d quark and a $\bar{c}$ quark. Since the $D^+(c\bar{d})$ does not have a quark in common with the beam, it cannot be produced the same way. Therefore, we expect an excess of D^- to D^+ mesons, especially at high x_F. This "leading particle effect" is clearly seen in the E791 data [1], as shown in Fig. 1. While the default version of PYTHIA predicts too much coalescence at low x_F, a modified ("tuned") version of PYTHIA provides good agreement with the data. The modifications included increasing the average intrinsic k_t of the partons from 0.44 GeV/c to 1.00 GeV/c and increasing the charm quark mass from 1.35 GeV/c^2 to 1.70 GeV/c^2.

In the case of the $\Lambda_c^+(udc)$, both particle and antiparticle share a quark with a $\pi^-(\bar{u}d)$. The target nucleons, however, share two quarks with the Λ_c^+ and none with the $\bar{\Lambda}_c^-$. Therefore, for π^-–nucleon interactions, we expect an increase in asymmetry as x_F decreases. The E791 data shown in Fig. 1 are consistent with an increase at x_F<0, as predicted by the default PYTHIA program. With these statistics, however, the data are also consistent with a flat asymmetry.

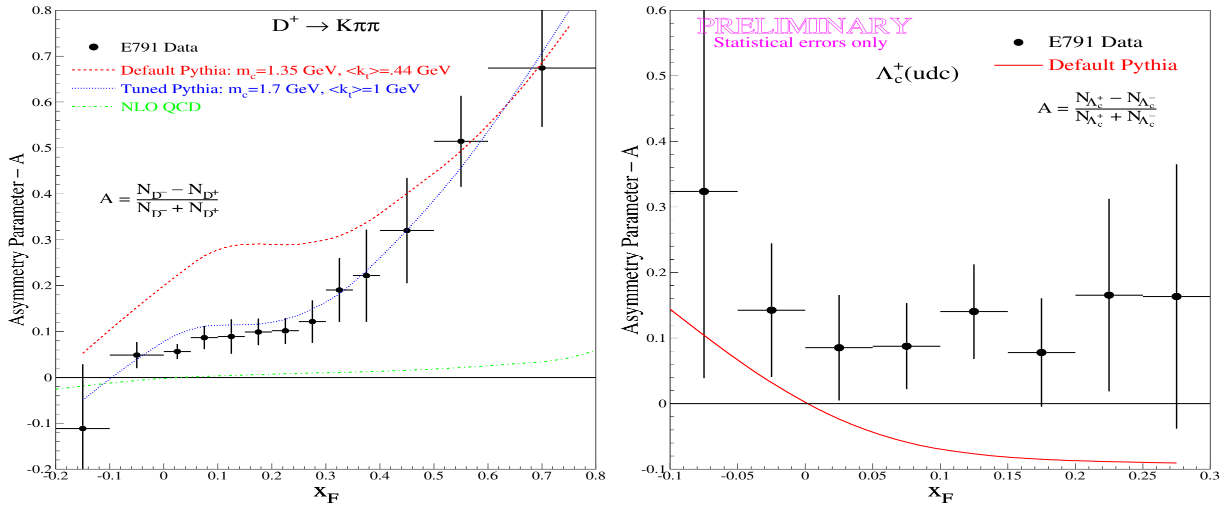

Figure 1: E791 results for $D^{\pm}$ and $\Lambda_c^{\pm}$ asymmetry versus x_F with a π^- beam.

SELEX has also measured the $D^{\pm}$ and $\Lambda_c^{\pm}$ asymmetries for Σ^-, π^-, and p beams. These asymmetries, shown in Fig. 2, are integrated over x_F>0.3. The slight Λ_c asymmetry with a π^- beam agrees with the E791 result. The large Λ_c asymmetries with baryon beams can be qualitatively understood using the beam dragging model. One puzzling observation, however, is that the p and Σ^- beams give the same Λ_c asymmetry even though the $p(uud)$ shares two quarks with the $\Lambda_c(udc)$ while the $\Sigma^-(dds)$ only shares one. The $D^{\pm}$ asymmetries with a π^- beam have the same sign as the E791 results for x_F>0.3 but are much less. The larger asymmetry from Σ^- produced $D^{\pm}$ compared to p produced $D^{\pm}$ is likely due to having more d quarks to choose from in the case of Σ^-.

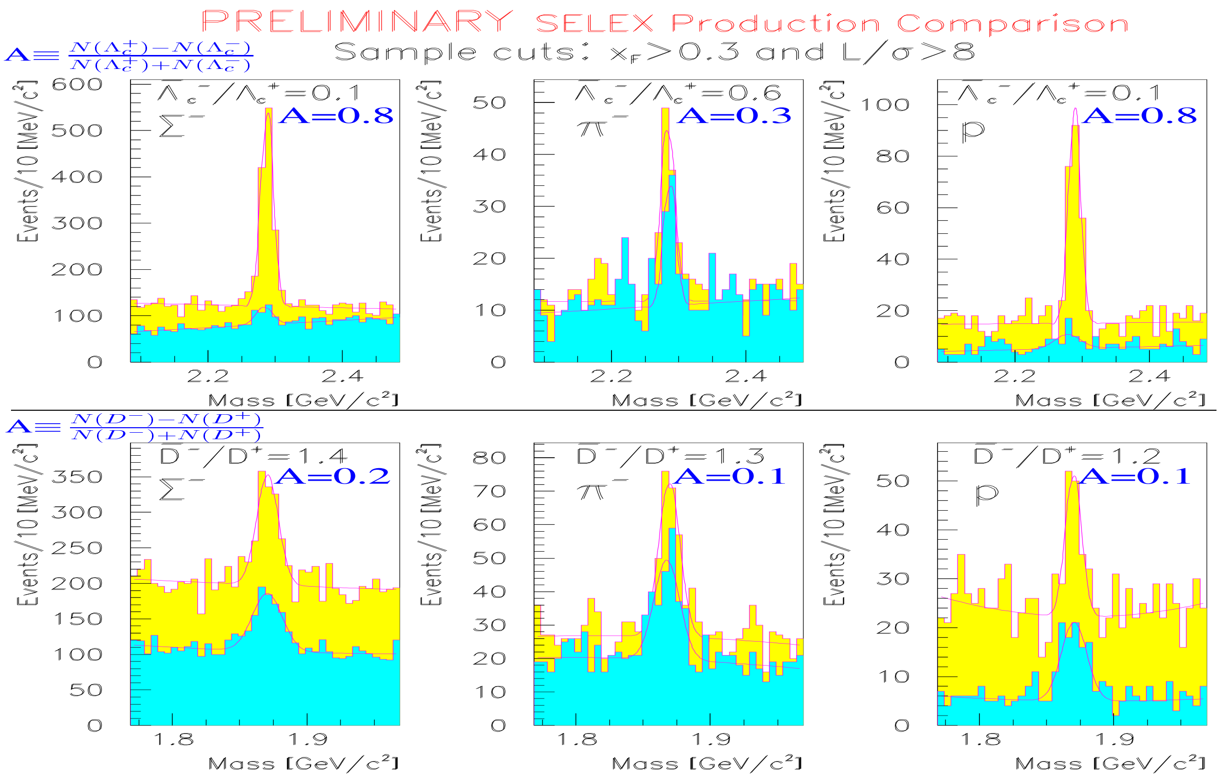

Figure 2: Preliminary SELEX results on $\Lambda_c^{\pm}$ and $D^{\pm}$ asymmetry at x_F>0.3 for Σ^-, π^-, and p beams.

FOCUS also has preliminary measurements of Λ_c asymmetries as a function of p_T^2 and p_L from 30% of their data (3397±90 Λ_c^+ and 2581±81 Λ_c^-), seen in Fig. 3. There is a clear positive asymmetry which favors Λ_c^+ production over Λ_c^- production. This is probably due to the larger availability of u and d quarks in the target fragments compared to $\bar{u}$ and $\bar{d}$ quarks. However, the kinematical dependence is still unclear. Analysis using the entire data set is ongoing.

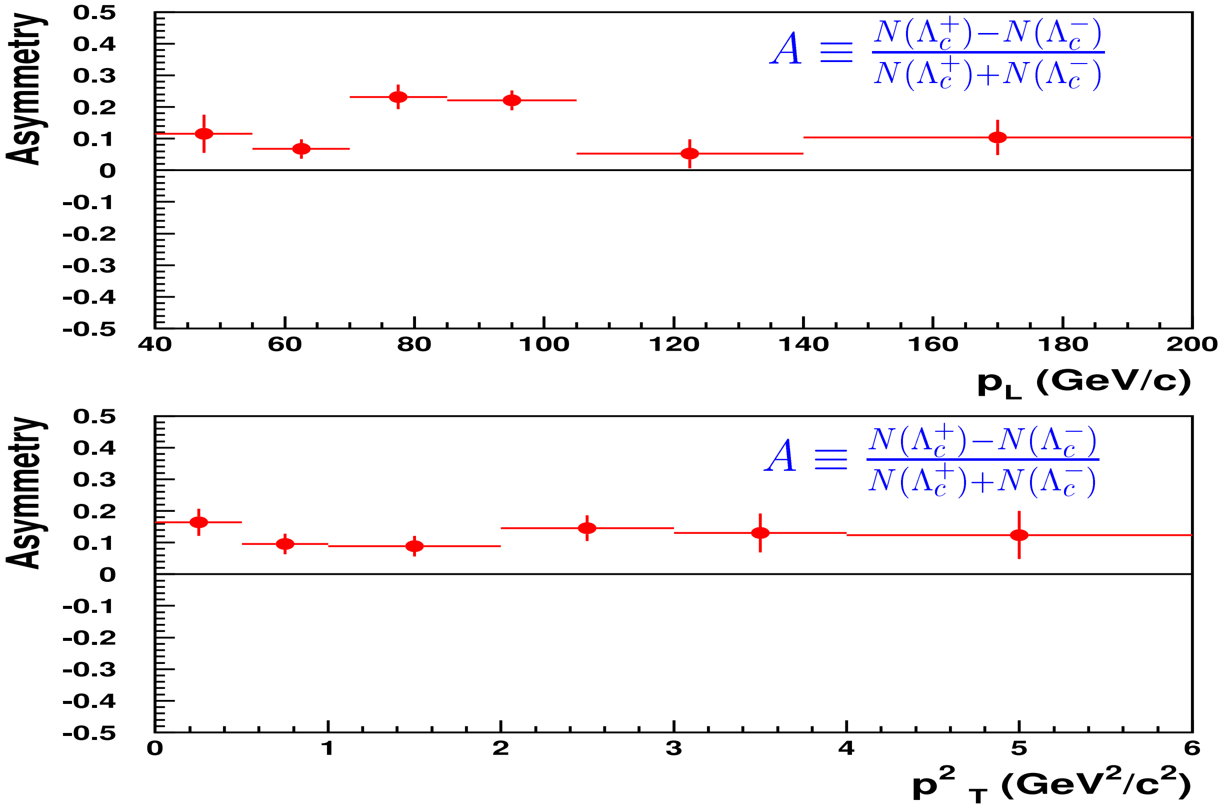

Figure 3: Preliminary FOCUS results based on 30% of the data showing the $\Lambda_c^\pm$ asymmetry versus longitudinal momentum and transverse momentum squared.

4 Charm-Pair Correlations

Charm-pair correlations allow one to measure aspects of the charm quark production as well as the hadronization. The correlations are obtained from events in which both the charm and anticharm particles are reconstructed. We can construct transverse correlations such as $\Delta\phi$, $\Delta p_t^2 \equiv |p_{t,D}^2 - p_{t,\overline{D}}^2|$, and $p_{t,D\overline{D}}^2 \equiv |\vec{p}_{t,D} + \vec{p}_{t,\overline{D}}|^2$. These correlations are sensitive to the charm quark production mechanism and relatively insensitive to hadronization effects.

Figure 4 shows the data sample for the E791 analysis[2] which finds 791±44 fully reconstructed charm-pair signal events. The azimuthal separation ($\Delta\phi$) distribution is also shown. The preliminary FOCUS result finds 7380±130 charm-paris signal events as seen in Fig. 5 along with the $\Delta\phi$ distribution. At leading order, $\Delta\phi = 180^o$, i.e. the charm particles are produced back-to-back. Higher order effects will smear out the delta function, however. Next-to-leading order[3] and PYTHIA[4] predictions for π^-–nucleon interactions are shown for comparison to the E791 results. These distributions actually provide a better match to the FOCUS results than the E791 results. The flatter $\Delta\phi$ distribution in the E791 results compared to the theoretical predictions and FOCUS results is most likely due to the more complicated hadronization process. Interestingly, both experiments appear to show a slight rise at $\Delta\phi \to 0$, perhaps due to diffractively produced charm or charm from gluon splitting.

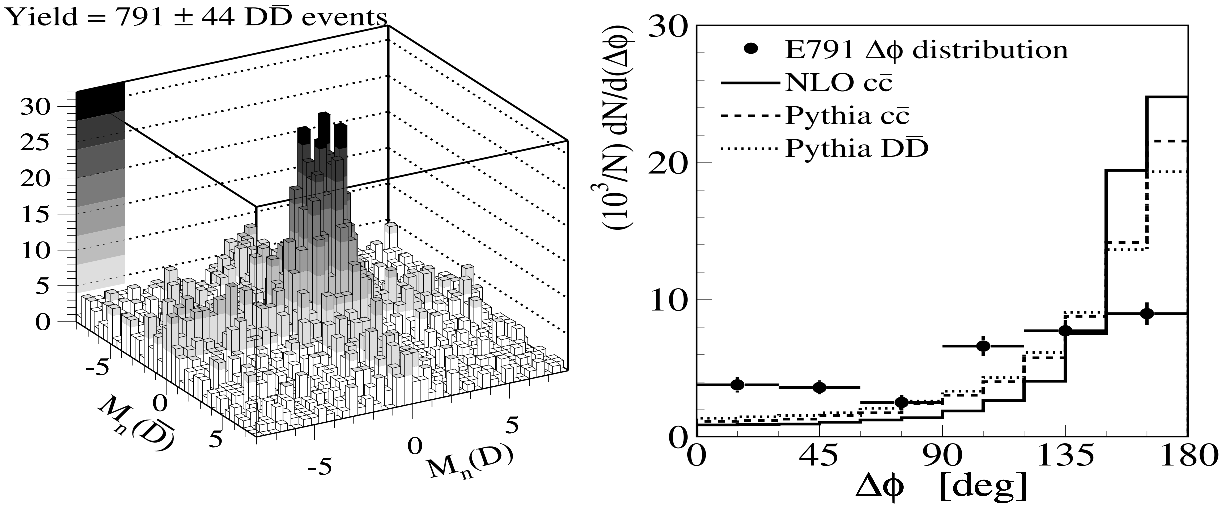

Figure 4: Plot of the D-candidate mass versus the $\overline{D}$-candidate mass for the charm-pair sample (left) and the acceptance corrected $\Delta\phi$ distribution from these events (right).

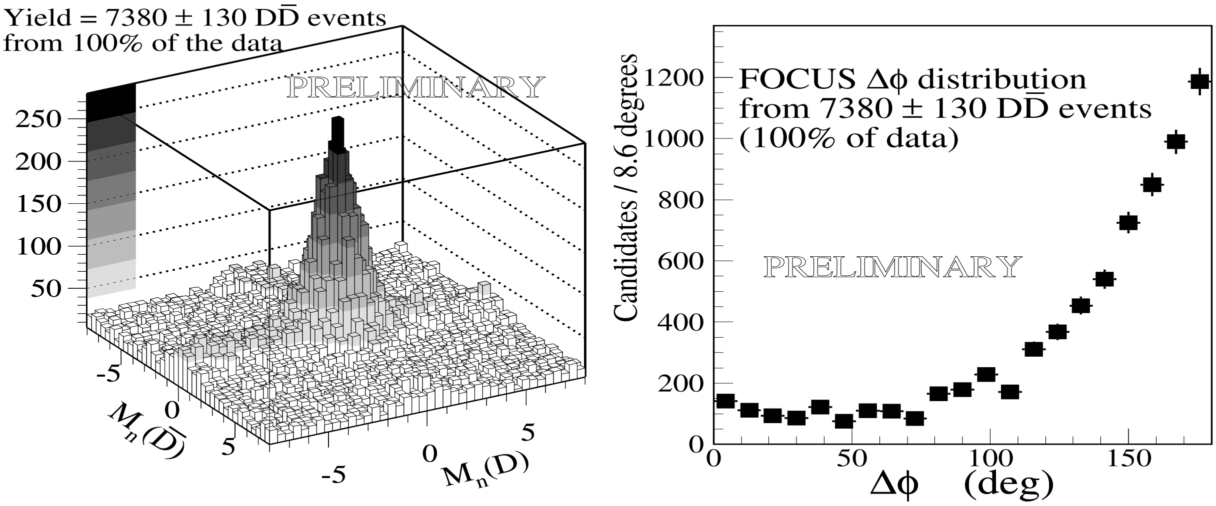

Figure 5: Plot of the FOCUS D-candidate mass versus the $\overline{D}$-candidate mass for the charm-pair sample (left) and the preliminary $\Delta\phi$ distribution from these events (right).

5 Differential Cross Sections

The differential cross sections are cross sections measured as a function of kinematic variables such as x_F and p_T^2. The shapes of these distributions are sensitive to both the charm quark production and the subsequent hadronization.

The preliminary SELEX results on the x_F distribution for Λ_c are shown in Fig. 6. Fitting the results to $(1-x_F)^n$, they find n values of 3.0±0.6, 3.5±0.4, and 2.7±0.2 for π^-, p, and Σ^- beams, respectively. All three of these results show a harder distribution (lower n) than D mesons where $n{\sim}4$–5. The fact that Λ_c^+ is a leading particle in all three case is probably the main contributor to this effect.

E791 has recently published results [5] on D^0 production from 88 990±460 $D^0 \to K\pi, K\pi\pi\pi$ events. Figure 7 shows the D^0 x_F and p_T^2 distributions along with fits to these distributions. The

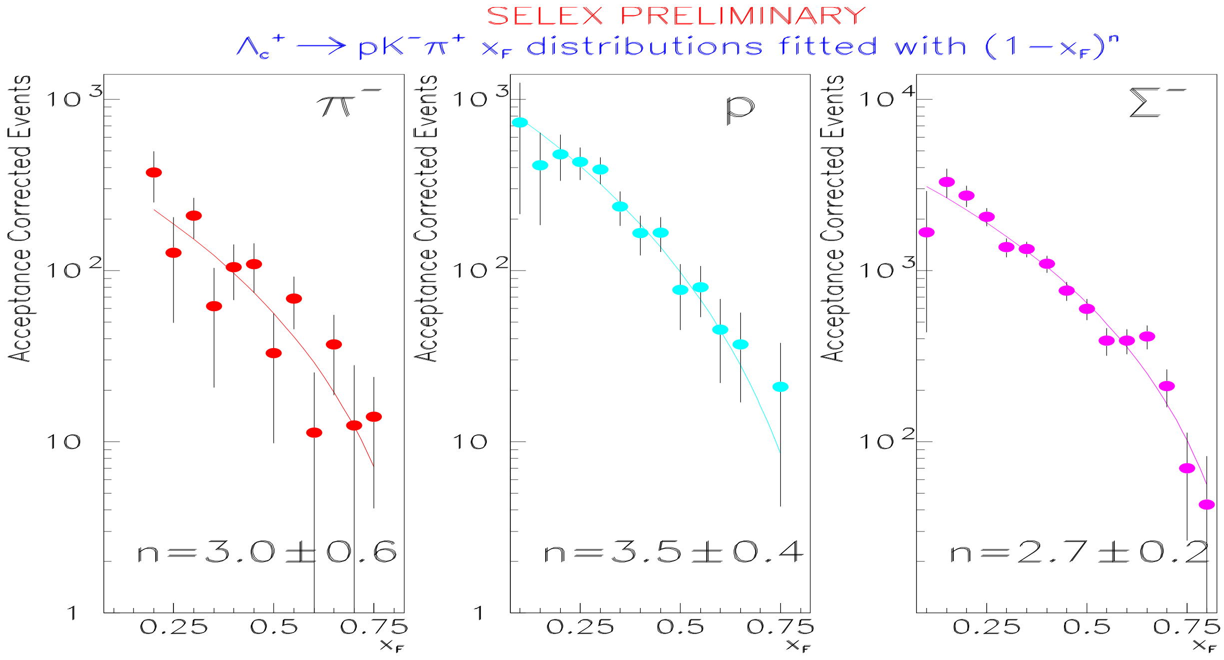

Figure 6: $D^{\pm}$ and $\Lambda_c^{\pm}$ x_F distributions for Σ^-, π^-, and p beams.

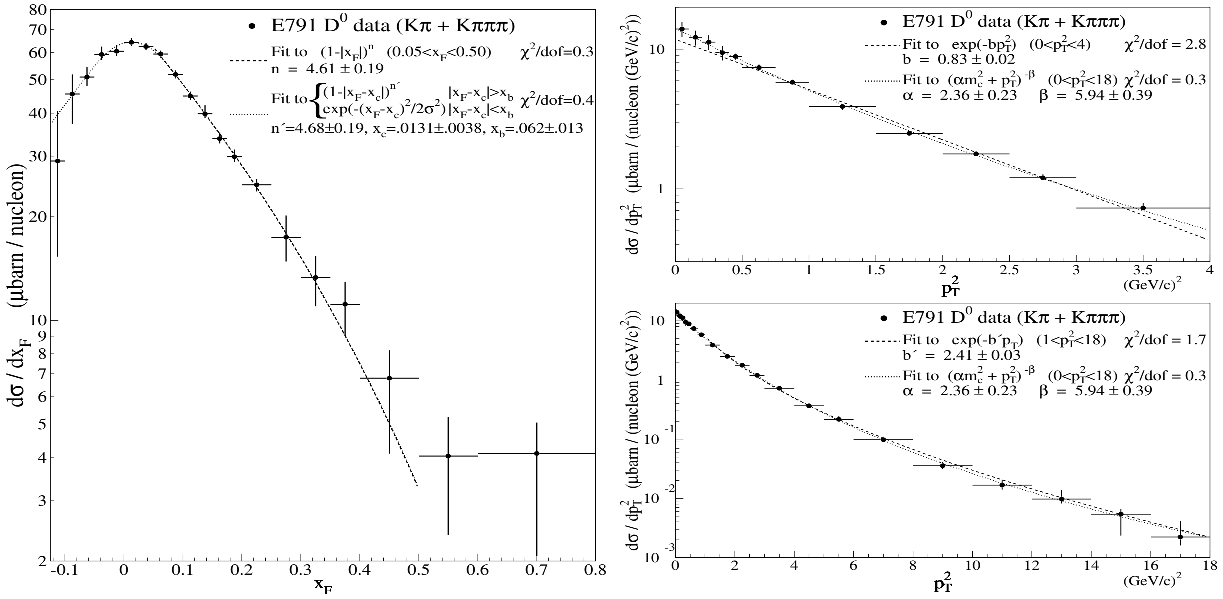

Figure 7: Fits to the E791 D^0+$\overline{D}^0$ x_F and p_T^2 (x_F>0) differential cross sections using the functions shown in the figures. Error bars do not include a $\sim \pm 10\%$ normalization uncertainty.

x_F distribution is fitted in the range -0.125<x_F<0.500 with the function

$$\frac{d\sigma}{dx_F} = \begin{cases} A(1-|x_F-x_c|)^{n'}, & |x_F-x_c| > x_b \\ A' \exp\left[-\frac{1}{2}(\frac{x_F-x_c}{\sigma})^2\right], & |x_F-x_c| < x_b \end{cases}. \tag{1}$$

The x_F turnover point, x_c, is found to be 0.0131±0.0038. The fact that it is significantly greater than zero is consistent with a harder gluon distribution in the beam pions than in the target nucleons. The n-value for these data is found to be 4.68±0.19. The high statistics also allow a good p_T^2 measurement out to 18 (GeV/c)^2.

Figure 8 shows a comparison of the E791 x_F and p_T^2 distributions to theoretical predictions for charm quark and D meson production. Although the data come from D^0 mesons, theoretical predictions for charm quark production are included for completeness. The theoretical curves are normalized to obtain the best fit to the data. The predictions come from the next-to-leading order (NLO) calculation [3] and the PYTHIA [4] event generator. The NLO charm quark calculation uses a charm quark mass of 1.5 GeV/c^2 and an average intrinsic transverse momentum of the incoming partons ($\sqrt{<k_t^2>}$) of 1.0 GeV/c. The D meson results are obtained by convoluting the charm quark results with the Peterson fragmentation function [6] with $\epsilon = 0.01$. The PYTHIA event generator uses a charm quark mass of 1.35 GeV/c^2, $\sqrt{<k_t^2>}$ of 0.44 GeV/c, and the Lund string fragmentation scheme to obtain D^0 results.

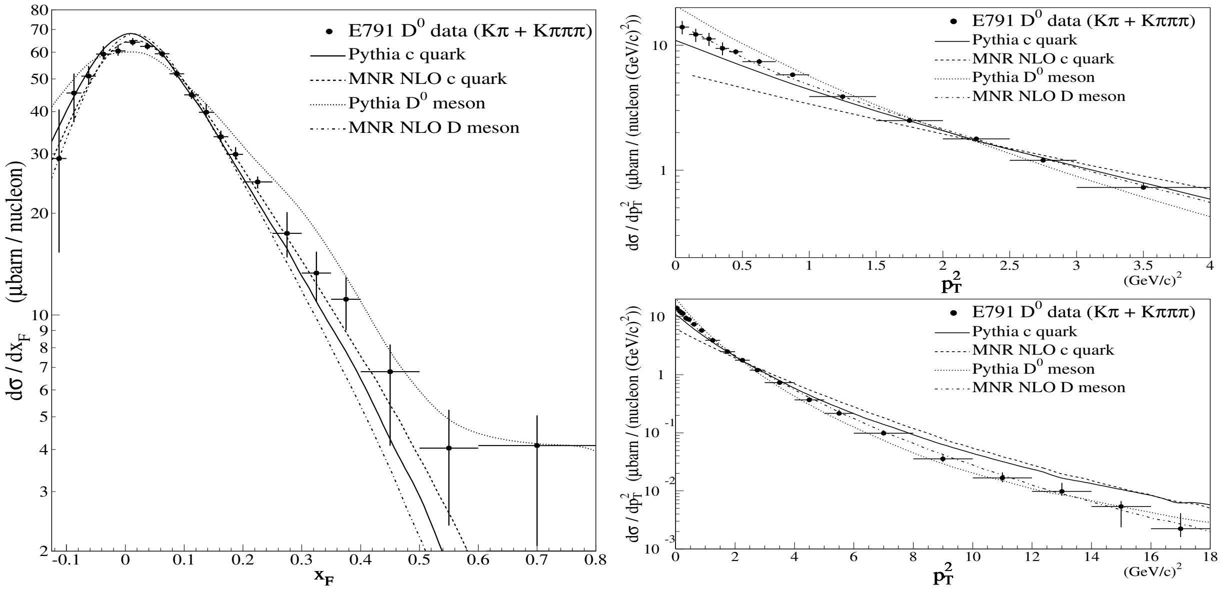

Figure 8: D^0+$\overline{D}^0$ x_F and p_T^2 (x_F>0) differential cross sections compared to next-to-leading order and PYTHIA predictions for c-quarks and D^0 mesons. Error bars do not include a $\sim \pm 10\%$ normalization uncertainty.

6 Total Cross Sections

E791 recently published results [5] on the charm total cross section. Assuming a linear dependence on the atomic number [7], they find a neutral-D total forward cross section, $\sigma(D^0 + \overline{D}^0; x_F > 0) = 15.4\ ^{+1.8}_{-2.3}$ μbarns/nucleon. To obtain the total charm cross section, the D^0+$\overline{D}^0$cross section is multiplied by 1.7 to account for three multiplicative effects: the relative production of charm quarks compared to D^0 mesons (2.1), the conversion from x_F>0 to all x_F (1.6), and the conversion to the $c\overline{c}$ cross section from the sum of charm plus anticharm cross sections (0.5) [8]. The total charm cross section from previous experimental results and the NLO prediction as a function of pion beam energy is shown in Fig. 9. Although the cross section energy dependence is modeled by the NLO theory, the absolute value depends greatly on the input parameters to the theory.

7 Conclusions

The field of charm production physics is difficult from both an experimental and theoretical perspective. Experimentally, the large statistics now available for differential and total cross section measurements pose a challenge to understanding the Monte Carlo with which one can obtain acceptance-corrected results. Reconstructing both charm candidates in an event, which is a sensitive probe of the charm quark production process, still suffers from a lack of statistics,

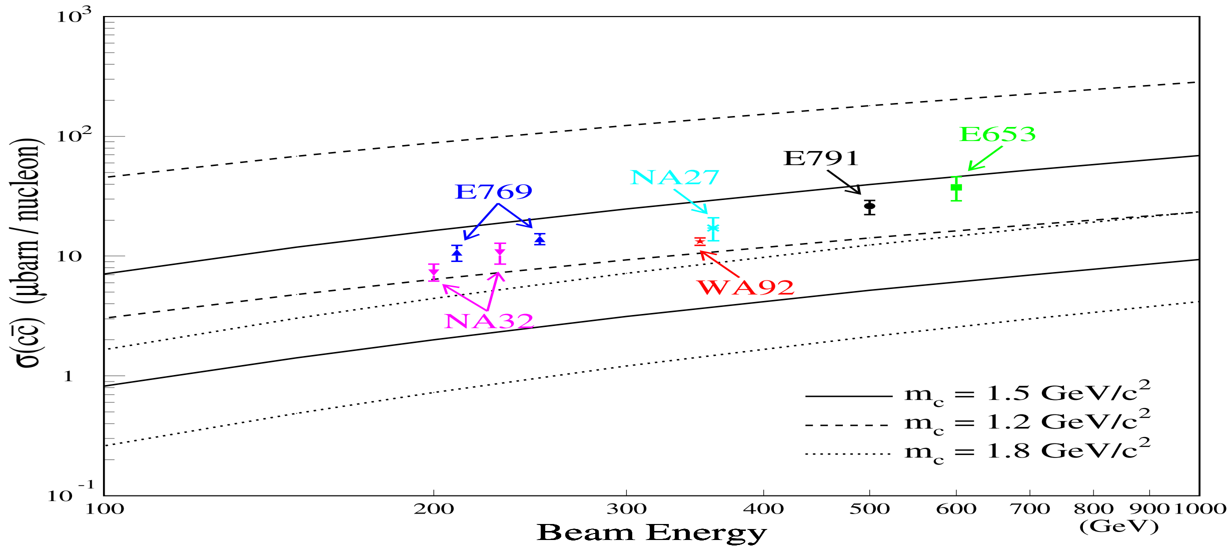

Figure 9: Theoretical and experimental results for the π–N $\to c\bar{c}$ cross section versus energy. The theoretical curves are obtained from NLO predictions [8]. The bands (solid, dashed, and dotted) correspond to different charm quark masses (1.5, 1.2, and 1.8 GeV/c^2). The variation within bands comes from varying the renormalization scale. The factorization scale is fixed. The E791 [5], E653 [9], NA27 [10], WA92 [11], NA32 (200 GeV) [12], NA32 (230 GeV) [13], and E769 [14] experimental data points are 1.7 times the single inclusive $D^0+\overline{D}^0$ $x_F>0$ cross sections.

however. FOCUS should advance this field with close to 10,000 charm-pair events, including $\Lambda_c D$ events. The theoretical challenges are even more severe. Perturbative QCD gives estimates of production variables for charm quarks with well understood errors. Converting to hadrons is a more difficult problem. Clearly, Peterson fragmentation is inherently unsuitable for hadron production environments since it can never reproduce the asymmetries seen by E791, SELEX, and FOCUS. A phenomenological approach such as the Lund string fragmentation model, while able to reproduce some of the asymmetries seen by E791, has its own problems including a large number of adjustable parameters and no mechanism for determining errors. The large theoretical uncertainties imply no single result, or even single experiment, can uniquely determine the physics of charm production or test QCD. However, combining the results of E791, FOCUS, and SELEX along with other past and future experiments may provide a coherent picture.

References

1. Aitala, E.M. *et al.*, E791 Collaboration, *Phys. Lett.* **B 371**, 157 (1996).
2. Aitala, E.M. *et al.*, E791 Collaboration, *Eur. Phys. J. direct* **C 4**, 1 (1999).
3. M.L. Mangano, P. Nason, and G. Ridolfi, *Nucl. Phys.* **B 405**, 507 (1993).
4. H.-U. Bengtsson and T. Sjöstrand, *Comp. Phys. Comm.* **46**, 43 (1987).
5. Aitala, E.M. *et al.*, E791 Collaboration, *Phys. Lett.* **B 462**, 225 (1999).
6. C. Peterson, D. Schlatter, I. Schmitt, and P. M. Zerwas, *Phys. Rev.* **D 27**, 105 (1983).
7. E769 Collaboration, G. A. Alves *et al.*, *Phys. Rev. Lett.* **70**, 722 (1993).
8. S. Frixione, M.L. Mangano, P. Nason, and G. Ridolfi, Heavy Flavours II, Advanced Series on Directions in High Energy Physics, 1997, hep-ph/9702287.
9. E653 Collaboration, K. Kodama *et al.*, *Phys. Lett.* **B B284**, 461 (1992).
10. LEBC-EHS Collaboration, M. Aguilar-Benitez *et al.*, *Phys. Lett.* **B 161**, 400 (1985).
11. BEATRICE Collaboration, M. Adamovich *et al.*, *Nucl. Phys.* **B 495**, 3 (1997).
12. ACCMOR Collaboration, S. Barlag *et al.*, *Z. Phys.* **C 39**, 451 (1988).
13. ACCMOR Collaboration, S. Barlag *et al.*, *Z. Phys.* **C 49**, 555 (1991).
14. E769 Collaboration, G. A. Alves *et al.*, *Phys. Rev. Lett.* **77**, 2388 (1996).